IEEE Access
Multidisciplinary | Rapid Review | Open Access Journal

Received November 22, 2021, accepted December 3, 2021, date of publication December 7, 2021,
date of current version January 4, 2022.

Digital Object Identifier 10.1109/ACCESS.2021.3133532

Fronthaul Optical Links Using Sub-Nyquist Sampling Rate ADC for B5G/6G Sub-THz Ma-MIMO Beamforming

PIN-HSUAN TING[1], SHAO-HUNG YU[2], ZHENG-WEI HUANG[1], CHIA-CHIEN WEI[3], (Member, IEEE), SIEN CHI[4], AND CHUN-TING LIN[4]

[1]Institute of Imaging and Biomedical Photonics, National Yang Ming Chiao Tung University, Tainan 11221, Taiwan
[2]Institute of Lighting and Energy Photonics, National Yang Ming Chiao Tung University, Tainan 11221, Taiwan
[3]Department of Photonics, National Sun Yat-sen University, Kaohsiung 80424, Taiwan
[4]Institute of Photonic System, National Yang Ming Chiao Tung University, Tainan 11221, Taiwan

Corresponding authors: Pin-Hsuan Ting (bingchen.cop08g@nctu.edu.tw) and Chun-Ting Lin (jinting@mail.nctu.edu.tw)

ABSTRACT This paper details fronthaul optical links using sub-Nyquist sampling rate analog-to-digital converters (ADCs) for Beyond fifth generation (B5G) and 6G sub-THz massive multiple-input multiple-output (Ma-MIMO) beamforming. Unlike Common Public Radio Interface (CPRI) using high speed ADCs in current fronthaul link, the proposed scheme involves ADCs operating at sub-Nyquist sampling rate for each antenna element. Based on pre-allocated relative time delays, pre-processed orthogonal frequency-division multiplexing (OFDM) signals sent from a baseband unit (BBU) can be deaggregated to different Ma-MIMO OFDM signals by sub-Nyquist sampling rate ADCs. In experiments, we assume that each remote radio unit (RRU) is equipped with 32/64 antenna elements and 32/64 ADCs operating at 1/32 and 1/64 of the Nyquist sampling rate. Furthermore, the received Ma-MIMO OFDM signal is then up-converted to 100-GHz for wireless transmission and defined as Ma-MIMO RF OFDM signal. We simulate the 32/64 antenna elements transmission scenario by individually transmit and demodulate each Ma-MIMO RF OFDM signal with 32/64 times of point-to-point antenna transmission. The error vector magnitude (EVM) and signal-to-noise ratio (SNR) of each received Ma-MIMO RF OFDM signal are less than 8% and 26 dB, respectively. And the total received 64 Ma-MIMO RF OFDM signals will require line rate as high as 393.6374 Gb/s according to CPRI option-7. Notably, the proposed scheme reduces the requirement of sampling rate and enables all the Ma-MIMO OFDM signals at baseband without the insertion of guard band. Thus, the proposed scheme can reduce the complexity of signal deaggregation and power consumption in the demodulation process, leading to an improvement in cost efficiency.

INDEX TERMS Sub-Nyquist, 5G, B5G, 6G, Massive multiple-input multiple-output (Ma-MIMO), sub-THz, THz, beamforming, fronthaul.

I. INTRODUCTION

From 4G to 5G mobile technologies, the data traffic has been increased 1000-fold due to proliferation of connected devices [1], and this trend is expected to continue in the next decade. Thus, how to provide more capacity in order to handle ever-increasing traffic has attracted considerable attention. There are a few key ways to increase the capacity, such as adding additional spectrum, equipping larger numbers of antennas, and putting up more cell cites. The aforementioned methods can be seen as general solution for network densification [2]. Compared to 5G, Beyond 5G (B5G)/6G would utilize more spectra, antennas (up to thousands) and cell cites to provide greater capacity and lower latency [3]. Moreover, B5G/6G will deploy sub-THz and THz bands to unleash its full potential for enabling new types of high-performance applications, such as 4K video streaming, reliable and latency-free automotive ecosystems, and internet of things (IoT). China Mobile Research Institute introduces Centralized-Radio Access Network (C-RAN) in 2010 and has become the key architecture concept in 5G networks and beyond. This concept breaks the base station

The associate editor coordinating the review of this manuscript and approving it for publication was Mohamed M. A. Moustafa.

equipment into two parts, the remote radio unit (RRU) and the baseband unit (BBU). The RRUs are equipped at the cell site towers and act as the wireless signal transceivers. On the other hand, the BBUs are aggregated into a central office, named BBU pool, with a joint controller to centralize the received/transmitted baseband signals and apply digital signal processing (DSP). The optical links, which interconnect the BBU and RRUs, are referred to as mobile fronthaul (MFH). Centralizing the BBUs brings several advantages such as flexible service deployment, joint processing, convenient maintenance and the potential to utilize 5G innovative technologies that require high processing power [4].

In order to meet the requirements of B5G/6G, one of the concerning issues is the use of Common Public Radio Interface (CPRI) between RRUs and BBUs, and changes have to be made to the MFH. According to the concept of digital radio-over-fiber (D-RoF), 4G LTE CPRI digitizes each LTE component carrier (CC) using a ADC with 30.72 MSa/s and 15 quantization bits. Referring to CPRI data rate option 2 [5], each LTE CC consumes 1.23-Gb/s fronthaul capacity. In order to increase the data rate, 3GPP release 10 standardized a technique named by carrier aggregation to aggregate 5 CCs together [6]. The number of aggregated CCs quickly expands to 32 by 3GPP release 13 [7], consuming up to 40-Gb/s fronthaul capacity when applying CPRI. Moreover, shifting operation bands into sub-THz/THz enables B5G/6G to transmit broadband wireless signals which require extremely high-speed Digital-to-Analog/Analog-to-Digital converters (DACs/ADCs) equipped at RRUs. As a result, CPRI and D-RoF structures become the data rate bottleneck of current MFH. On the other hand, transmitting optical signal in analog form will significantly improve the spectral efficiency of MFH, and the architecture is called Analog RoF (A-RoF). Analog MFH based on A-RoF has the advantages of simple, low-cost implementations and high spectral efficiency. Analog MFH integrated with DSP-enabled carrier aggregation [8], [9] and analog carrier aggregation [10] has been experimentally demonstrated. However, problems of high-speed ADC and complex DSP still remain.

There are various novel technologies such as artificial intelligence (AI), massive multiple-input multiple-output (Ma-MIMO), THz communications, dynamic network slicing and beamforming (BF) that have been investigated as potential enablers of B5G/6G [11]. The sub-THz/THz channels suffer from extremely high propagation loss and sensitivity to blockage. In order to compensate for the propagation loss and leverage the short wavelengths of sub-/THz, B5G/6G MFH will support Ma-MIMO systems with hundreds or even thousands of antennas. Furthermore, beamforming (BF) technique combined with the Ma-MIMO system can improve space-division multiplexing and spectral efficiency [12]. However, each antenna element requires one Radio frequency (RF) chain in the fully digital BF structure. When applying Ma-MIMO systems, the number of antenna (N_{AE}) is very large. Thus, the high cost and high-resolution ADCs and DACs make fully digital BF hard to implement. In [13], a promising analog solution for fronthaul integrating with Ma-MIMO systems are proposed. However, the architectures proposed in [13] would require analog filters for deaggregating individual signals (for example, 128 filters for 128 signals). Also, the use of analog filters might not provide enough flexibility and scalability to meet the requirement of dynamic B5G/6G networks. In [14], a subcarrier multiplexing DSP-assisted A-RoF structure which applies both discrete multi-tone signals and single sideband modulation signals as the multiplexing method for each channel are proposed. However, additional frequency guard bands are essential for the multiplexing method in the distributed unit, and the digital filters are also required in the remote radio unit to deaggregate the signals. Compared with [14], our proposed structure only needs simple LSR-ADC for deaggregation. Hence, the complexity of RRU would not severely increase with the number of aggregated signals. For the concern of hardware cost, researches have been conducted on RF chain reduction for MIMO systems, such as hybrid BF structure [15], [16]. The requiring number of RF chain (N_{RF}) for hybrid BF and digital BF to have equal spectral efficiency (bits/s/Hz) are shown in Fig.1 according to [16].

Our proposed structure focuses on dealing with the MFH capacity and high-speed ADC issues. In this study, we use 7-GHz-bandwidth intensity-modulation and direct-detection (IM-DD) channel to support 64 RF chains sub-band signals (164.0156 Hz). After 10-km single mode fiber (SMF) transmission, each RF chain signal is down-sampled by 1/64 Nyquist-sampling rate to obtain Ma-MIMO RF OFDM signal, and the error vector magnitude (EVM) of each RF chain is less than 8%. Furthermore, this work experimentally demonstrates a 100-GHz 1.5-m wireless transmission to support 64 RF chains without adding additional overhead, and the structure can be easily integrated with Ma-MIMO systems. According to CPRI option-7, the total received 64 Ma-MIMO RF OFDM signals will require line rate as high as 393.6374 Gb/s ($=64 \times 2 \times 15 \times 164.0156 \times 10.8$ Mb/s) which cannot be achieved with current MFH structure.

The rest of this paper is organized as follows. Section II introduces the concept of A-RoF MFH using DDM-OFDM Scheme. In Section III, the experimental setup is carefully discussed. Section IV shows experimental results. Finally, conclusions are drawn in Section V.

II. SYSTEM MODEL

Fig. 2 shows the schematic diagram of DSP-assisted analog RoF (DSP-A-RoF), which was adopted in [14], and our proposed system. At RRU, the DSP-A-RoF receives the aggregated signal and uses a high-speed ADC to enable deaggregation using DSP. After deaggregating the signal, each CC occupies different frequency band and makes it difficult to integrate with beamforming. Therefore, all the CCs need to be down-converted to the baseband, necessitating additional processing. These above-mentioned DSP procedures will increase the complexity and total cost of RRU, making it less suitable for the Ma-MIMO system in

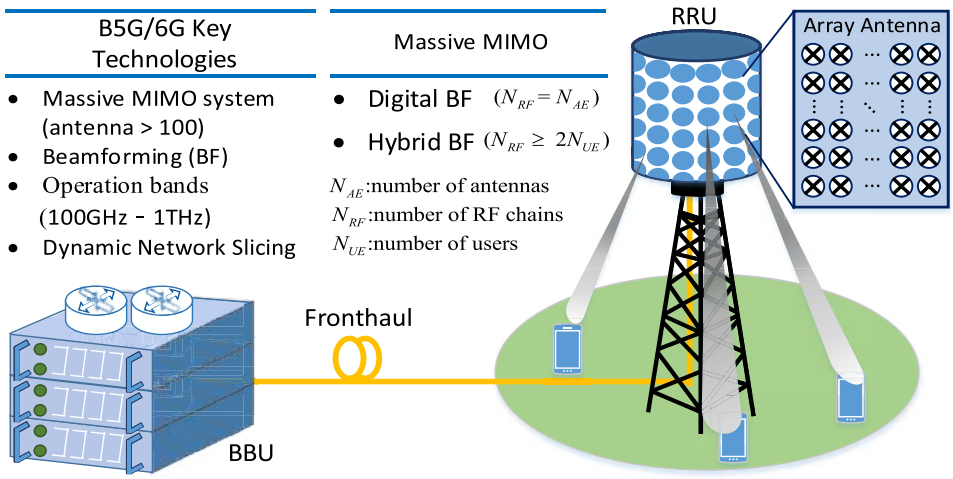

FIGURE 1. B5G/6G MFH deploys Massive MIMO systems equipped with N_{AE} antennas.

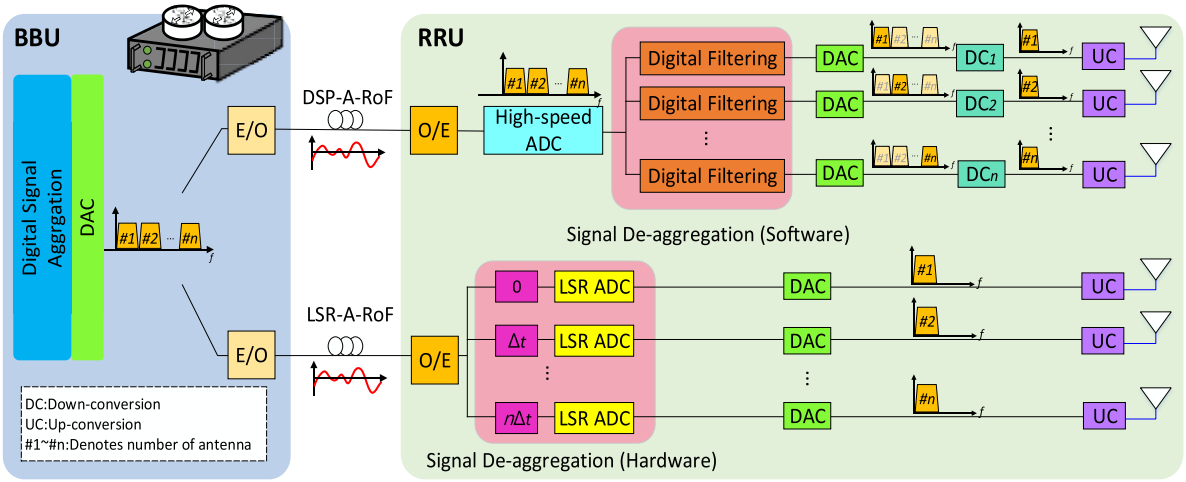

FIGURE 2. The schematic diagram of DSP-assisted analog RoF (DSP-A-RoF) and our proposed system. The digital filtering will cause extra latency. According to different center frequency, the up-conversion and down-conversion need to be applied individually making it tedious for practical implement.

B5G/6G systems. Besides, the high-speed ADC is still a large financial burden of Ma-MIMO systems when applying wide-band signal transmission. By contrast, our proposed analog MFH equipped with low-sampling-rate ADCs (LSR-ADCs) can simplify the structure of RRU. By preprocessing the total OFDM signal, the LSR-ADC deaggregates the total OFDM signal into different Ma-MIMO RF OFDM signals cooperated with proper delay times. Moreover, our proposed MFH enables all the Ma-MIMO RF OFDM signals at baseband without the insertion of guard band comparing with a general A-RoF system. The requirement of extremely high-speed ADC is an issue in B5G/6G wired and wireless communication systems. In fact, several systems using LSR-ADCs based on the delay-division-multiplexing (DDM) scheme have been demonstrated to alleviate the burden of high-speed ADC [17], [18]. Different from previous works, where users and LSR-ADCs are distributed at different locations. The users in Ma-MIMO RRU scenario are in the same wireless network coverage area and so as the LSR-ADCs. Hence, the time-synchronization will be easier for the Ma-MIMO RRU scenario. This paper proposed a novel B5G/6G MFH links based on the DDM scheme with LSR-ADCs. We successfully demonstrated both high capacity analog MFH and 100-GHz wireless systems. Moreover, the DDM concept can obtain all signals at the baseband, thereby reducing the per-signal processing at the RRU. This would be beneficial in Ma-MIMO RRU scenario, where more than hundreds of signals are aggregated to provide enough data rate for B5G/6G networks. Generally, the OFDM scheme follows the Nyquist sampling theory in order to prevent spectral aliasing. However, the DDM scheme takes the opposite view by defining aliasing as a predictable phenomenon and considers the OFDM subcarriers received by LSR-ADC as a linear combination of particular subcarriers. In our proposed

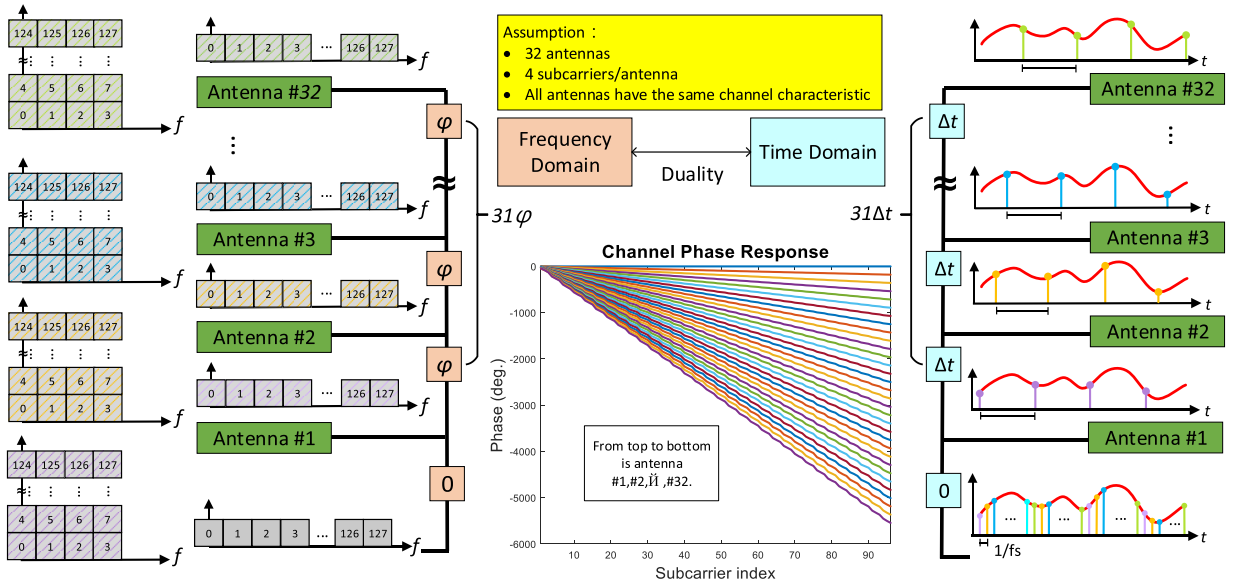

FIGURE 3. Concept of DDM-OFDM analog MFH.

DDM scheme, OFDM subcarriers are divided equally into M parts, and each part belongs to an antenna. Compared to the general OFDM scheme, our proposed system only requires an LSR-ADC with $1/M$ Nyquist sampling rate. Fig. 3 shows the concept of proposed DDM-OFDM scheme integrated with MFH, and the parameters in this example are set as $M = 32$ and $N = 128$, where M, N and N/M denotes the number of antennas, subcarrier number at the transmitter and that received by each group, respectively. The subcarriers received by each group are the linear combination of the sent subcarriers in our proposed scheme. Moreover, different delay times cause different phase slopes in the frequency domain, as shown in Fig. 3; hence, the received subcarriers received by different LSR-ADC could be different. In other words, we can control each signal of antenna by manipulating the delay time when receiving the signal. It should be noted that M can be further extended to 64 or even hundreds of antennas in order to support the huge Ma-MIMO system. Under the assumption that all the antennas have the same channel characteristics, the effects of transmission and aliasing can be represented as

$$\mathbf{HS} = \mathbf{R} \rightarrow \begin{bmatrix} \mathbf{H}_{0,0} & \mathbf{H}_{0,1} & \cdots & \mathbf{H}_{0,M-1} \\ \mathbf{H}_{1,0} & \mathbf{H}_{1,1} & \cdots & \mathbf{H}_{1,M-1} \\ \vdots & \vdots & \ddots & \vdots \\ \mathbf{H}_{M-1,0} & \mathbf{H}_{M-1,1} & \cdots & \mathbf{H}_{M-1,M-1} \end{bmatrix} \times \begin{bmatrix} S_0 \\ S_1 \\ \vdots \\ S_{N-1} \end{bmatrix} = \begin{bmatrix} \mathbf{R}_0 & \mathbf{R}_1 & \ldots & \mathbf{R}_{M-1} \end{bmatrix}^{\mathrm{T}} \quad (1)$$

where

$$\mathbf{H}_{m,\dot{m}} = \begin{bmatrix} H_{m,\frac{\dot{m}N}{M}} & 0 & \cdots & 0 \\ 0 & H_{m,\frac{\dot{m}N}{M}+1} & \cdots & 0 \\ \vdots & \vdots & \ddots & \cdots \\ 0 & 0 & \vdots & H_{m,\frac{\dot{m}N}{M}+\frac{N}{M}-1} \end{bmatrix} \quad (2)$$

$$\mathbf{R}_m = \begin{bmatrix} R_{m,0} & R_{m,1} & R_{m,2} & \ldots & R_{m,\frac{N}{M}-1} \end{bmatrix}^{\mathrm{T}} \quad (3)$$

$\mathbf{H}$, $\mathbf{S}$ and $\mathbf{R}$ denote the channel responses, transmitted OFDM subcarriers and the received OFDM subcarriers aggregated from all RRUs. $H_{m,n}$ indicates the channel response of the $(n+1)$th sent subcarrier for the $(m+1)$th group; $\mathrm{S_n}$ indicates the $(n+1)$th transmitted subcarrier; $\mathbf{R}_m$ and $\mathrm{R}_{m.l}$ indicate all of the subcarriers and the $(l+1)$th subcarrier received by the $(m+1)$th group, where $m \in \{0, 1, \ldots, M-1\}$ and $l \in \{1, 2, \ldots, (N/M)-1\}$. Notably, $\mathbf{H}$ includes the phase responses generated by delays and the effect of spectral aliasing. As the example shown in Fig. 3, owing to the sub-Nyquist sampling, each received subcarrier is comprised of 32 transmitted subcarriers. The difference between initial sampling time of receivers is multiple Δt; i.e. $m\Delta t$, where $m = 0, 1, 2, \ldots, 31$ for antenna 1,2, $\ldots$,32 in Fig. 3, respectively. Thus the induced phase of the n-th subcarrier would be $n\omega \times m\Delta t$, where $\omega/(2\pi)$ is equal to the subcarrier spacing. Comparing to normal OFDM scheme with equal total bandwidth, sampling rate, and FFT size, our DDM-OFDM scheme have better SNR performance, as shown in Fig. 5, due to the ability of pre-equalization in the preprocessing procedure. Hence, in accordance with the desired received signals $\mathbf{R}$, the sent signal can be modified as $\mathbf{S} = \mathbf{H}^{-1}\mathbf{R}$, such that no additional DSP is needed thanks to $\mathbf{HS} = \mathbf{H}\left(\mathbf{H}^{-1}\mathbf{R}\right) = \mathbf{R}$ (note that $\mathbf{H}$ is invertible). Consequently, each RRU in our

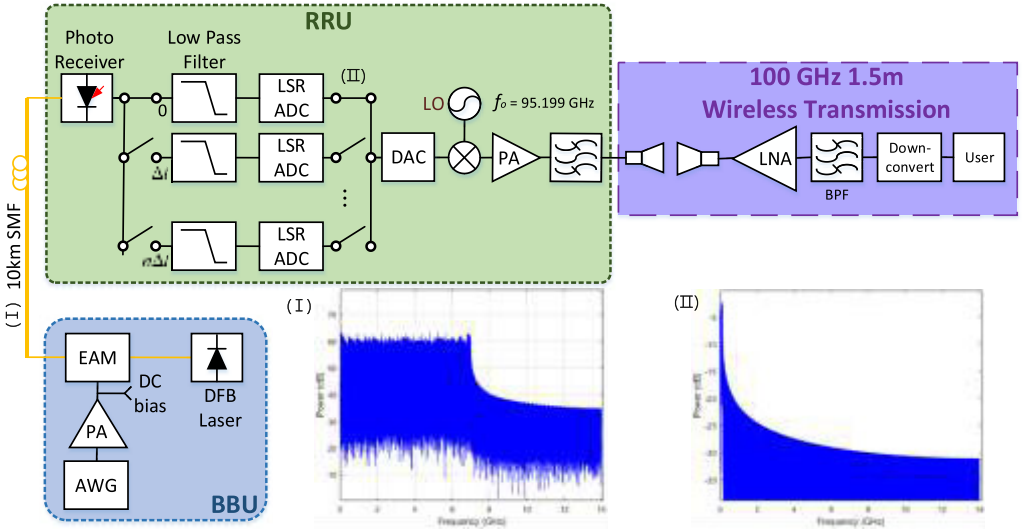

FIGURE 4. Experimental setup for MFH and wireless transmission. (I) Total OFDM signal spectrum. (II) Ma-MIMO OFDM signal spectrum received by LSR-ADC.

proposed scheme only requires an LSR-ADC with $1/M$ Nyquist sampling rate without the need for down conversion.

III. EXPERIMENTAL SETUP

Fig. 4 shows the experiment setup of the proposed MFH link equipped with LSR-ADC and the 100-GHz 1.5m wireless transmission. For proof-of-concept experiments, we emulate LSR-ADCs by DSP. We generated the preprocessed 64 QAM OFDM signal by an arbitrary waveform generator (AWG, Keysight M8195A) with DAC sampling rate of 28-GSample/s, and the total bandwidth was equal to 6.998-GHz, as shown in Fig. 4 (I). The FFT size, subcarrier number, and frequency spacing were set as 2048, 1024, and 6.83 MHz, respectively. Hence, the Nyquist sampling rate of the total bandwidth is 13.98 GSample/s. The total OFDM signal was transmitted through 10 km SMF to simulate the MFH link between BBU and RRU. In the RRU, the LSR-ADC equally divided the total OFDM signals into 64 Ma-MIMO RF OFDM signals according to corresponding delay time, and the electric spectrum is as shown in Fig. 4 (II). Notably, the band width of Ma-MIMO OFDM signal spectrum received by LSR-ADC would vary according to number of antennas. In Fig. 4, the band width of each Ma-MIMO OFDM signal can be represented as $B_{\mathrm{Ma-MIMO}} = 6.998/64 = 0.1093(\mathrm{GHz})$. Finally, each Ma-MIMO OFDM signal was up-converted to 100-GHz for wireless transmission, and defined as Ma-MIMO OFDM RF signal. Notably, compared with traditional A-RoF system, our proposed MFH links enable all the Ma-MIMO OFDM signals without the insertion of guard band and located at baseband.

The EVM requirements of 16QAM and 64QAM have been specified by 3GPP release 12 [19], which are 12.5% and 8%, respectively. Fig. 5 presents the 16QAM BTB EVM curve of OFDM and our proposed scheme, while the number of antennas is set as 1, 8, 32, and 64. Fig. 6 presents EVM curves

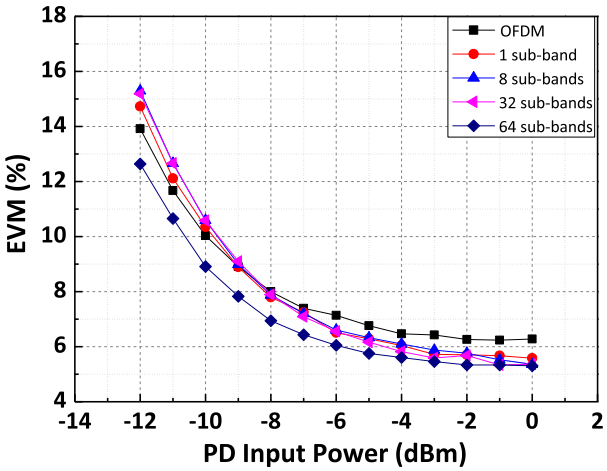

FIGURE 5. EVM curve of 16QAM BTB.

with the modulation format of 64QAM and the other parameters remain the same. Fig. 5 and 6 reveal that our proposed scheme has almost no penalty comparing to OFDM. Moreover, we can enlarge the number of antennas from 1 to 64 without EVM penalty, which is suitable for integrated with Ma-MIMO system. Then, 64QAM was used to test the transmission over 10-km SMF. The measured EVM curves are shown in Fig.7. Our proposed scheme has the ability to support up to 64 RRUs without significant EVM penalty according to Fig. 5-7. Compared with 4G LTE CPRI, the line rate needed for our proposed scheme in option-7 is as high as 393.6374 Gb/s ($64 \times 2 \times 15 \times 164.0156 \times 10.8$ Mb/s), which is very challenging without the proposed scheme.

IV. EXPERIMENTAL RESULTS AND DISCUSSION

In this section, we evaluate the performance of the proposed MFH link equipped with LSR-ADC and the 100-GHz 1.5m wireless transmission. There are four transmission scenarios

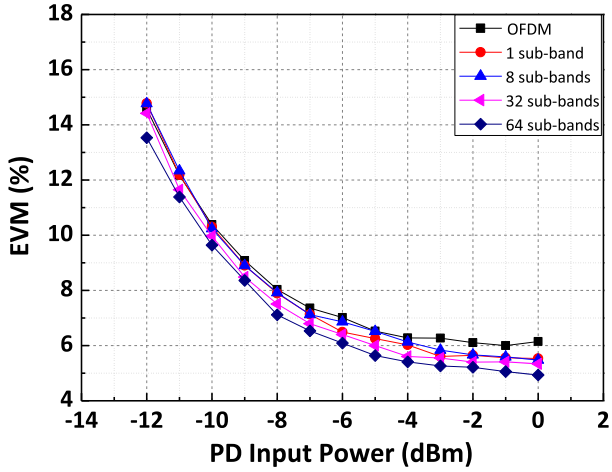

FIGURE 6. EVM curve of 64QAM BTB.

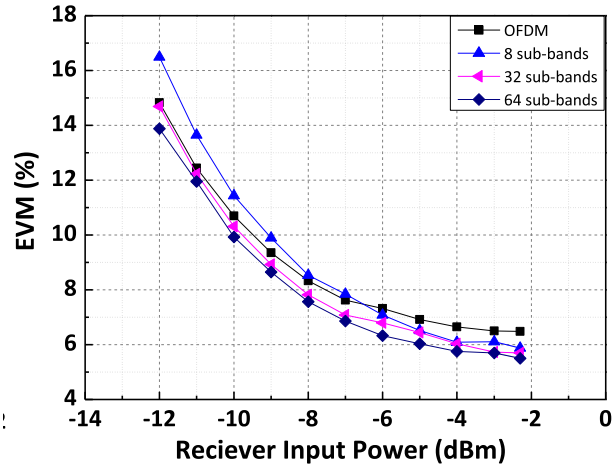

FIGURE 7. EVM curve of 64QAM 10-km fronthaul link.

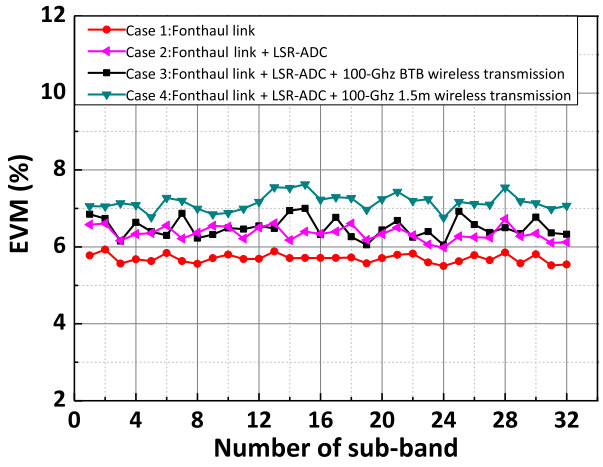

FIGURE 8. EVM curve of 32-antennas scenario.

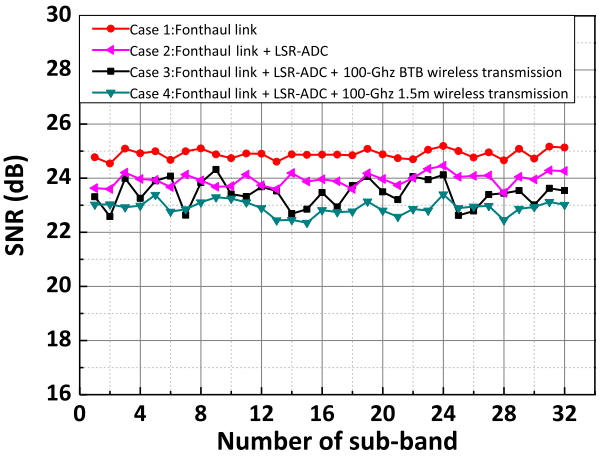

FIGURE 9. SNR curve of 32-antennas scenario.

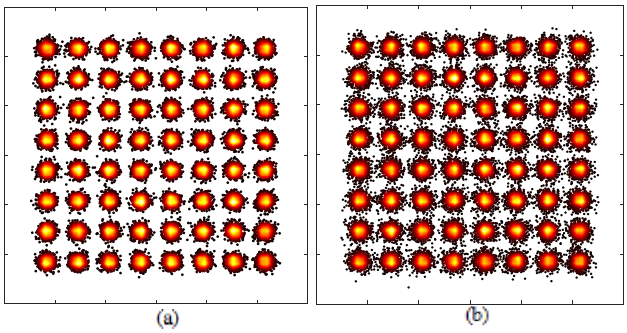

FIGURE 10. (a) Constellation of 32-antennas fronthaul link. (b) Constellation of 32-antennas 100-GHz 1.5m wireless transmission.

in the investigation: the simulation of fronthaul link, fronthaul link with LSR-ADC transmission, fronthaul link with LSR-ADC and 100-GHz BTB wireless transmission, and fronthaul link with LSR-ADC and 100-GHz 1.5m wireless transmission referred to as case 1-4 in Fig.8 and 9, respectively. In case 1, we transmit the total OFDM signal through 10 km SMF to simulate the transmission between BBU and RRH. For proof-of-concept experiments, we use LSR-ADC which is realized by oscilloscope and DSP to separate the total OFDM signal into M Ma-MIMO OFDM signals. Then the received M Ma-MIMO OFDM signals through BTB experiment denotes as case 2. In case 3, we up-convert each Ma-MIMO OFDM to 100-GHz which is defined as Ma-MIMO RF OFDM signal and set the distance between Tx antenna and Rx antenna as 0m. Finally, Tx antenna and Rx antenna are separated by a distance of 1.5 m and we transmit each Ma-MIMO RF OFDM signal individually. Fig.8 and 9 show the EVM and SNR curves of four types of transmission link in 32-antennas scenario. As the result, the EVM penalty between the case 1 and case 2 comes from the additional transmission between the AWG and the oscilloscope. Comparing the case 2 and case 3, we can observe that the up-conversion generate almost no penalty to our proposed scheme. The case 4 shows the EVM and SNR of each received Ma-MIMO RF OFDM signal

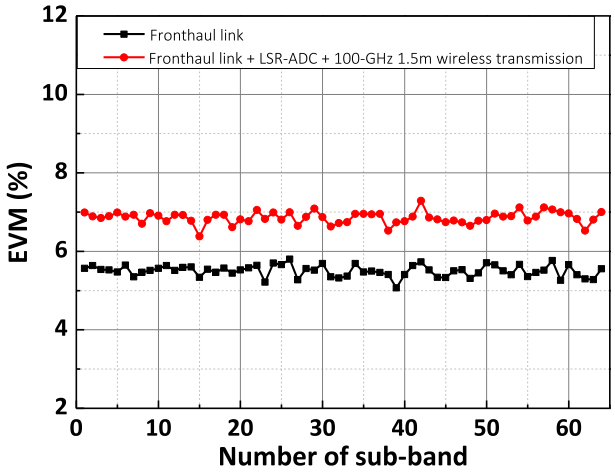

FIGURE 11. EVM curve of 64-antennas scenario.

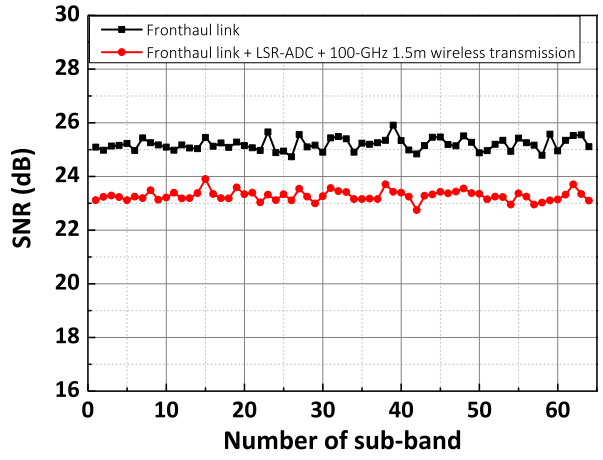

FIGURE 12. SNR curve of 64-antennas scenario.

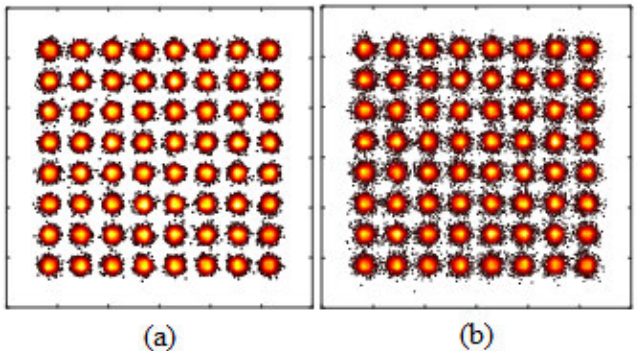

FIGURE 13. (a) Constellation of 64-RRUs fronthaul link. (b) Constellation of 64-antennas 100-GHz 1.5m wireless transmission.

underneath 8% and 26 dB, respectively. The constellation of fronthaul link (10-km SMF) and the overall fronthaul link with 1.5-m wireless transmission in 32-antennas scenario are shown in Fig.10(a)(b). Furthermore, Fig.11 and 12 show that our proposed scheme can support the number of antennas up to 64 without penalty. The constellation of fronthaul link and the overall fronthaul link with 1.5-m wireless transmission in 64-antennas scenario are shown in Fig.13(a)(b). Theoretically, we can extend the number of antennas up to 128 or even 256 to support the B5G/6G Ma-MIMO system. Moreover, our proposed scheme enables all the Ma-MIMO OFDM signals without the insertion of guard band and located at baseband will be suitable for integrating HBF technology.

V. CONCLUSION

We propose a 7-GHz IM-DD channels with 1/64 Nyquist-sampling-rate ADCs and low computational complexity without extra hardware. The corresponding CPRI Option-7 capacity needs to be 393.6374 Gb/s. Notably, compared with traditional A-RoF system, our proposed MFH links with simple structure enable all the Ma-MIMO OFDM signals without the insertion of guard band and located at baseband. Moreover, comparing to general OFDM scheme, our proposed scheme has better performance when the number of antennas extends to 32 and 64 as shown in Fig.7, which is suitable for future B5G/6G Ma-MIMO MFH. All the EVMs among 32 or 64 antennas are almost equal to or less than 8%, implying the feasibility of employing the beamforming technology.

ACKNOWLEDGMENT

The authors are thankful to Dr. Chia-Chien Wei and Chun-Ting Lin for their precious comments and suggestions which are very helpful to improve the quality of the paper.

REFERENCES

[1] J. Zander and P. Mähönen, "Riding the data tsunami in the cloud: Myths and challenges in future wireless access," *IEEE Commun. Mag.*, vol. 51, no. 3, pp. 145–151, Mar. 2013.
[2] B. Romanous, N. Bitar, A. Imran, and H. Refai, "Network densification: Challenges and opportunities in enabling 5G," in *Proc. IEEE 20th Int. Workshop Comput. Aided Modelling and Design Commun. Links Netw. (CAMAD)*, Sep. 2015, pp. 129–134.
[3] P. Yang, Y. Xiao, M. Xiao, and S. Li, "6G wireless communications: Vision and potential techniques," *IEEE Netw.*, vol. 33, no. 4, pp. 70–75, Jul./Aug. 2019.
[4] I. A. Alimi, A. L. Teixeira, and P. P. Monteiro, "Toward an efficient C-RAN optical fronthaul for the future networks: A tutorial on technologies, requirements, challenges, and solutions," *IEEE Commun. Surveys Tuts.*, vol. 20, no. 1, pp. 708–769, 1st Quart., 2018.
[5] *Common Public Radio Interface (CPRI) Specification V7.0*. Accessed: Oct. 9, 2015. [Online]. Available: http://www.cpri.info/downloads/CPRI_v_7_0_2015 10 09.pdf
[6] *Evolved Universal Terrestrial Radio Access (E-UTRA);Carrier Aggregation; Base Station (BS) Radio Transmission and Reception*, document V. 3GPP TR36.808, 2013.
[7] *New WI Proposal: LTE Carrier Aggregation Enhancement Beyond 5 Carriers*, document 3. RP142286, 2014.
[8] X. Liu, F. Effenberger, N. Chand, L. Zhou, and H. Lin, "Demonstration of bandwidth-efficient mobile fronthaul enabling seamless aggregation of 36 E-UTRA-Like wireless signals in a single 1.1-GHz wavelength channel," in *Proc. Opt. Fiber Commun. Conf.*, 2015.
[9] X. Liu, H. Zeng, N. Chand, and F. Effenberger, "Efficient mobile fronthaul via DSP-based channel aggregation," *J. Lightw. Technol.*, vol. 34, no. 6, pp. 1556–1564, Mar. 15, 2016.
[10] M. Zhu, X. Liu, N. Chand, F. Effenberger, and G. K. Chang, "High-capacity mobile fronthaul supporting LTE-advanced carrier aggregation and 8×8 MIMO," in *Proc. Opt. Fiber Commun. Conf. (OFC)*, 2015.

[11] M. Z. Chowdhury, M. Shahjalal, S. Ahmed, and Y. M. Jang, "6G wireless communication systems: Applications, requirements, technologies, challenges, and research directions," *IEEE Open J. Commun. Soc.*, vol. 1, pp. 957–975, 2020.
[12] L. Yu, J. Wu, A. Zhou, E. G. Larsson, and P. Fan, "Massively distributed antenna systems with nonideal optical fiber fronthauls: A promising technology for 6G wireless communication systems," *IEEE Veh. Technol. Mag.*, vol. 15, no. 4, pp. 43–51, Dec. 2020.
[13] L. Cheng, X. Liu, N. Chard, F. Effenberger, and G. K. Chang, "Experimental demonstration of sub-nyquist sampling for bandwidth-and hardware-efficient mobile fronthaul supporting 128×128 MIMO with 100-MHz OFDM signals," in *Proc. Opt. Fiber Commun. Conf.*, Mar. 2016, p. W3C-3.
[14] S. Noor, P. Assimakopoulos, and N. J. Gomes, "A flexible subcarrier multiplexing system with analog transport and digital processing for 5G (and Beyond) fronthaul," *J. Lightw. Technol.*, vol. 37, no. 14, pp. 3689–3700, Jul. 15, 2019.
[15] T. Gong, N. Shlezinger, S. S. Ioushua, M. Namer, Z. Yang, and Y. C. Eldar, "RF chain reduction for MIMO systems: A hardware prototype," *IEEE Syst. J.*, vol. 14, no. 4, pp. 5296–5307, Dec. 2020.
[16] K. Roth, H. Pirzadeh, A. L. Swindlehurst, and J. A. Nossek, "A comparison of hybrid beamforming and digital beamforming with low-resolution ADCs for multiple users and imperfect CSI," *IEEE J. Sel. Topics Signal Process.*, vol. 12, no. 3, pp. 484–498, Jun. 2018.
[17] C.-C. Wei, H.-C. Liu, C.-T. Lin, and S. Chi, "Analog-to-digital conversion using sub-nyquist sampling rate in flexible delay-division multiplexing OFDMA PONs," *J. Lightw. Technol.*, vol. 34, no. 10, pp. 2381–2390, May 15, 2016.
[18] S. H. Yu, P. -Y. Huang, C. -H. Lin, C. -T. Lin, C. C. Wei, and S. Chi, "Broadband wired and wireless access system with novel sub-nyquist sampling-rate ADC receiver," in *Proc. Opto-Electron. Commun. Conf. (OECC)*, Oct. 2020, pp. 1–2.
[19] *Summary of 3GPP TSG-RAN Workshop on Release 12 and Onward*. document 3GPP RWS-120045. [Online]. Available: https://www.3gpp.org/ftp/workshop/2012-06-11_12_RAN_REL12/Docs/RWS120045.zip

PIN-HSUAN TING received the B.S. degree in electrical engineering from National Tsing Huang University, Hsinchu, Taiwan. She is currently pursuing the M.S. degree with the Institute of Imaging and Biomedical Photonics, National Yang Ming Chiao Tung University, Tainan, Taiwan. Her research interests include image processing, machine learning, and hybrid beamforming.

SHAO-HUNG YU received the B.S. degrees in photonics from National Sun Yat-sen University, Kaohsiung, Taiwan. He is currently pursuing the M.S. degree with the Institute of Lighting and Energy Photonics, National Yang Ming Chiao Tung University, Tainan, Taiwan. His research interests include organic material synthesis, free space optics, and communication systems.

ZHENG-WEI HUANG received the B.S. degree in electro optical engineering from National United University, Miaoli, Taiwan. He is currently pursuing the M.S. degree with the Institute of Imaging and Biomedical Photonics, National Yang Ming Chiao Tung University, Tainan, Taiwan. His research interests include non-linear compensation, machine learning, and communication systems.

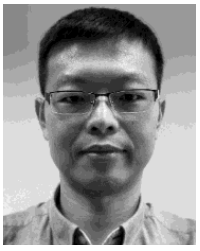

CHIA-CHIEN WEI (Member, IEEE) received the Ph.D. degree in electro-optical engineering from National Chiao Tung University, Hsinchu, Taiwan, and the Electrical Engineering degree from the University of Maryland, Baltimore, MD, USA, in 2008. In 2011, he joined National Sun Yat-sen University, Kaohsiung, Taiwan, where he is currently a Professor with the Department of Photonics. His current research interests include optical and electrical signal processing, advanced modulation formats, optical access networks, and radio-over-fiber systems.

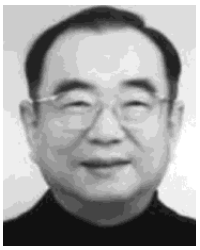

SIEN CHI received the B.S.E.E. degree from National Taiwan University, Taipei, Taiwan, in 1959, the M.S.E.E. degree from National Chiao Tung University, Hsinchu, Taiwan, in 1961, and the Ph.D. degree in electrophysics from Polytechnic Institute, Brooklyn, NY, USA, in 1971. From 1971 to 2004, he was a Professor with National Chiao Tung University. From 1998 to 2001, he was the Vice President of National Chiao Tung University. He is currently a Chair Professor with National Chiao Tung University. His research interests include optical-fiber communications, fast and slow light, passive optical networks, and microwave photonics. He is a fellow of the Optical Society of America.

CHUN-TING LIN received the B.S. and M.S. degrees in material science and engineering from National Tsing Huang University, Hsinchu, Taiwan, in 1997 and 2001, respectively, and the Ph.D. degree in electro-optical engineering from National Yang Ming Chiao Tung University, Hsinchu, in 2007. His research interests include radio-over-fiber systems, optical data formats, and optoelectronic packages.